

# Wheel tread defect detection for high-speed trains using FBG-based online monitoring techniques

Xiao-Zhou Liu<sup>1,2a</sup> and Yi-Qing Ni<sup>\*1,2</sup>

<sup>1</sup>Hong Kong Branch of Chinese National Rail Transit Electrification and Automation Engineering Technology Research Center, Hong Kong

<sup>2</sup>Department of Civil and Environmental Engineering, The Hong Kong Polytechnic University, Hung Hom, Kowloon, Hong Kong

(Received December 29, 2017, Revised March 29, 2018, Accepted March 31, 2018)

**Abstract.** The problem of wheel tread defects has become a major challenge for the health management of high-speed rail as a wheel defect with small radius deviation may suffice to give rise to severe damage on both the train bogie components and the track structure when a train runs at high speeds. It is thus highly desirable to detect the defects soon after their occurrences and then conduct wheel turning for the defective wheelsets. Online wheel condition monitoring using wheel impact load detector (WILD) can be an effective solution, since it can assess the wheel condition and detect potential defects during train passage. This study aims to develop an FBG-based track-side wheel condition monitoring method for the detection of wheel tread defects. The track-side sensing system uses two FBG strain gauge arrays mounted on the rail foot, measuring the dynamic strains of the paired rails excited by passing wheelsets. Each FBG array has a length of about 3 m, slightly longer than the wheel circumference to ensure a full coverage for the detection of any potential defect on the tread. A defect detection algorithm is developed for using the online-monitored rail responses to identify the potential wheel tread defects. This algorithm consists of three steps: 1) strain data pre-processing by using a data smoothing technique to remove the trends; 2) diagnosis of novel responses by outlier analysis for the normalized data; and 3) local defect identification by a refined analysis on the novel responses extracted in Step 2. To verify the proposed method, a field test was conducted using a test train incorporating defective wheels. The train ran at different speeds on an instrumented track with the purpose of wheel condition monitoring. By using the proposed method to process the monitoring data, all the defects were identified and the results agreed well with those from the static inspection of the wheelsets in the depot. A comparison is also drawn for the detection accuracy under different running speeds of the test train, and the results show that the proposed method can achieve a satisfactory accuracy in wheel defect detection when the train runs at a speed higher than 30 kph. Some minor defects with a depth of 0.05 mm~0.06 mm are also successfully detected.

**Keywords:** wheel condition monitoring; wheel tread defect; track-side sensing system; FBG strain gauge arrays; outlier analysis

## 1. Introduction

Wheel defects or out-of-roundness (OOR) can give rise to severe damage on vehicle components and track structure (Johansson and Nielsen 2003), including rail fatigue, rail joint deterioration, sleeper degradation and failure, service life reduction of wheels and bearings (Barke and Chiu 2005), especially when the trains run at high speeds (Morys 1999). Besides, impact excited by defective wheel can increase the noise intensity (Pettersson 2000, Wu and Thompson 2002). The causes of wheel defects including wheel flats and wheel polygonization (periodic out-of-roundness) are so complex that they may occur unpredictably and have been found on trains operating on many lines with very different operation conditions. To

solve the problem and ensure safety operation, railway authorities generally adopt wheel reprofiling (wheel lathing) as a common and effective approach to eliminating wheel defects. Wheel reprofiling is always conducted following a mileage-based schedule for each multiple unit train. A problem thus arises: in wheel reprofiling, all the wheelsets of an electric multiple unit (EMU) including those without defects will be subject to maintenance which might result in shortening of the service life of the healthy wheelsets (Lagnebäck 2007). It is thus important to narrow the coverage of wheel reprofiling to the faulty wheels only based on an effective method to screen out the wheels with defects before reprofiling.

Aiming at wheel defect detection, a lot of research has been carried out on the modeling of wheel-rail dynamic interaction based on different contact models (Nielsen and Oscarsson 2004, Ding *et al.* 2014, Baeza *et al.* 2006, Pieringer *et al.* 2014, Yang and Thompson 2014). Finite element methods for rail and wheel simulation were also used (Zhao *et al.* 2011, Bian *et al.* 2013) to investigate the dynamic response on wheel or rail structure influenced by wheel defects. But very few studies focused on developing

\*Corresponding author, Professor  
E-mail: [yiqing.ni@polyu.edu.hk](mailto:yiqing.ni@polyu.edu.hk)

<sup>a</sup> Ph.D., Research Associate

online wheel condition monitoring systems.

Online monitoring can be more effective than offline/static inspection for wheel condition assessment and defect detection (Barke and Chiu 2005, Ni 2015). Compared with the vehicle-borne wheel defect detection method (Wei and Chen 2013) and accelerometer-based detector (Müller-BBM 2015), the track-side wheel impact load detector (WILD) can be more suitable for large quantity of wheel inspections because the strain response can be directly linked to wheel impact (Ding *et al.* 2016). The sensors in impact detection system are usually the strain gauge rosettes (Milković *et al.* 2013, Asplund *et al.* 2014) or fiber Bragg grating (FBG) sensors (Wei *et al.* 2012, Filograno *et al.* 2013) which are especially suitable for strain monitoring of structures (Zhang *et al.* 2014, Ye *et al.* 2017). But the adaptability of WILD to high-speed trains still needs further investigations and the defect identification methods based on wheel impact load monitoring data may need further development, especially in minor defect detection or when the passage trains run at low speeds.

This paper develops an FBG-based track-side WILD for wheel local defect detection. The detector, as an online rail response monitoring system, consists of two FBG strain gauge arrays installed on the rail foot of a pair of rails, an interrogator for data collection, and a computer for system control and data storage. After obtaining the rail response monitoring data from all the FBGs along both arrays, a three-step process based on outlier analysis is used for potential defect detection of wheels. To validate the proposed method, an 8-car EMU equipped with wheelsets with artificial local defects was chosen as the test train. It ran 20 times at different speed levels of 10, 20, 30, 40 and 50 kph (4 runs for each level). By applying the proposed defect detection method, it is found that the detection results agree well with the results from the offline wheel tread inspection conducted in the depot, even when the defect depth is as low as 0.05~0.06 mm.

## 2. FBG-based track-side wheel condition monitoring system

### 2.1 Rail dynamic response monitoring

This study uses the FBG-based sensing technology to develop a track-side WILD for potential wheel tread defects. It was found in our previous study (Ni *et al.* 2017) that the impact caused by wheel defect will generate novel responses on the rail, so a strain gauge mounted on the rail can collect response data that may reflect potential wheel defect. Also, because the location of wheel defect excitation on the rail head is randomly distributed with a period of the wheel tread perimeter, a dense sensor array installed on the rail can be used to detect local defect(s) on the wheel tread if the length of the array is not shorter than the wheel tread perimeter. The interval can be determined by the identifiability of the novel response features.

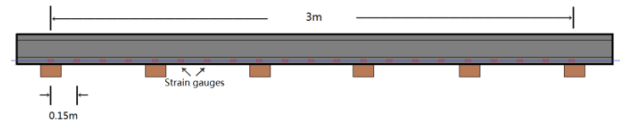


Fig. 1 Deployment of FBG strain gauge arrays

### 2.2 Layout of FBG arrays

To detect potential local defect(s) on the wheel tread, we design an FBG strain gauge array that can be mounted at the rail foot along the longitudinal direction. The length of the array is around 3 m, which is slightly longer than the circumference of the wheel tread and the interval of the FBGs along the array is 0.15 m. This can ensure that no less than three FBGs can sense the novel response features when a potential defect hits at any location within the instrumented rail segment. Each FBG can measure the longitudinal strain of rail foot caused by bending moment of the cross-section under the excitation of the wheel impact. The layout consists of two arrays mounted on a pair of rails, as shown in Fig. 1. The output rail bending moment can then be obtained as

$$M_i = \frac{EI}{y} \varepsilon_i = \frac{EI}{Ky} \Delta\lambda_i, \quad i = 1, 2, \dots, N_s \quad (1)$$

where  $M_i$  is rail cross sectional bending moment at location  $i$ ;  $EI$  the flexural rigidity;  $y$  the height difference between the neutral axis and the sensor array;  $K$  the sensitivity coefficient of FBG;  $\Delta\lambda_i$  the wavelength change of the  $i$ th FBG installed on the rail; and  $N_s$  the number of FBGs on the array.

### 2.3 System configuration

As shown in Fig. 2, The proposed wheel load detector consists of: 1) two FBG strain gauge arrays installed on the foot of a pair of rails, as described in Sub-section 2.1; 2) a high-speed interrogator; and 3) a computer with data acquisition software. As a wheel load detector, the monitoring system collects monitoring data of rail responses at a sampling rate of 5000 Hz and is triggered to store data during train passage automatically. Because the transmission distance of a fiber optic sensing system can be as long as 100 km, the interrogator as a data logger can be positioned with computer in a control room far away from the instrumented rail section.

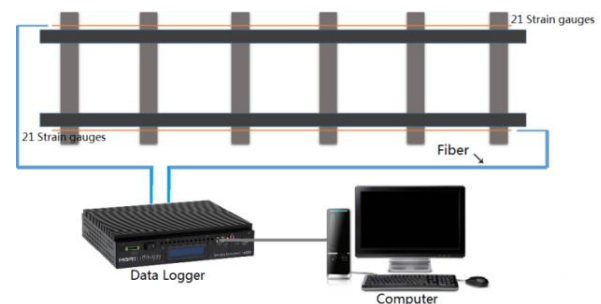


Fig. 2 Online wheel load detector for wheel condition monitoring

### 3. Wheel defect detection using online monitoring data of rail response

#### 3.1 General description

The process of wheel defect detection based on monitoring data of rail responses can be divided into three steps, as shown in Fig. 3.

Step 1: this step is to conduct data pre-processing for the subsequent wheel defect detection. In this step, the amplitude and location of response peaks are picked up from the time history of monitoring data, as shown in Fig. 4. The global rail response collected by different FBGs along the arrays excited by each wheel can be extracted, as shown in Fig. 5(a). The Savitzky-Golay (S-G) filter is used to normalize the response data and the normalized data, as shown in Fig. 5(b), will be used to detect potential defects. The data normalization method will be detailed in Sub-section 3.2.

Step 2: this step primarily conducts outlier analysis based on Chauvenet’s criterion to find novel response in the time history of the normalized response data for all of the passage wheelsets. If no novel response resulting from the excitation of the  $i$ th wheel is found, the outlier analysis will proceed to the  $(i+1)$ th wheel. The outlier analysis will be detailed in Sub-section 3.3.

Step 3: this step is a refined analysis for the novel responses found in Step 2, targeting to detect potential defects. When the outlier dataset is not empty (i.e., the dataset contains novel responses), the novel responses and their features will be subject to further investigation. If in an outlier dataset there are no less than three novel responses (collected by different FBGs at the same time period), the novel responses in the outlier dataset are likely those generated by the excitation of a potentially defective wheel. The features of the potential defect, including the relative response amplitude and its location on the wheel tread, can then be obtained subsequently. The identification procedure of wheel defect will be detailed in Sub-section 3.4.

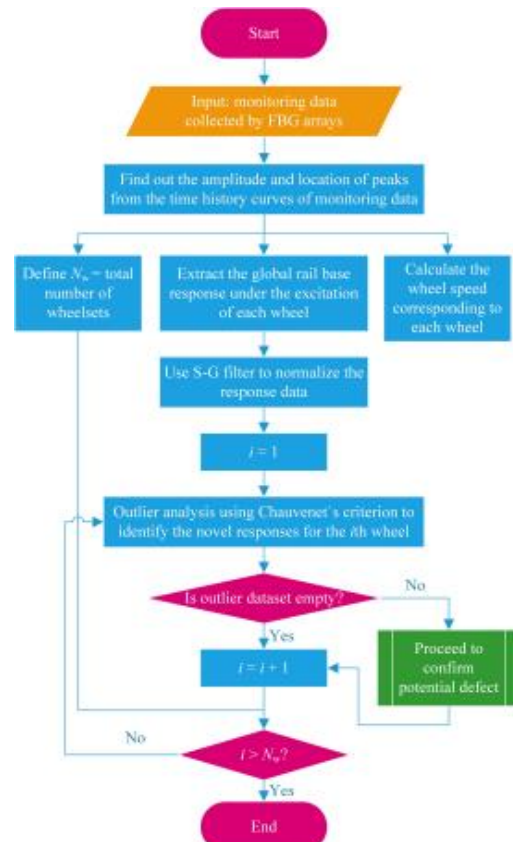
#### 3.2 Data normalization

The original strain response of one FBG at rail base under the excitation of an 8-car EMU (32 wheels) is shown in Fig. 4. The time history of the strain response contains 32 peaks corresponding to 32 wheels. To identify the defective wheel, the roughness of all the wheel treads should be examined through analyzing the corresponding peak signals collected by all FBGs. Fig. 5 shows the strain data collected by an FBG array under the excitation of the same wheel.

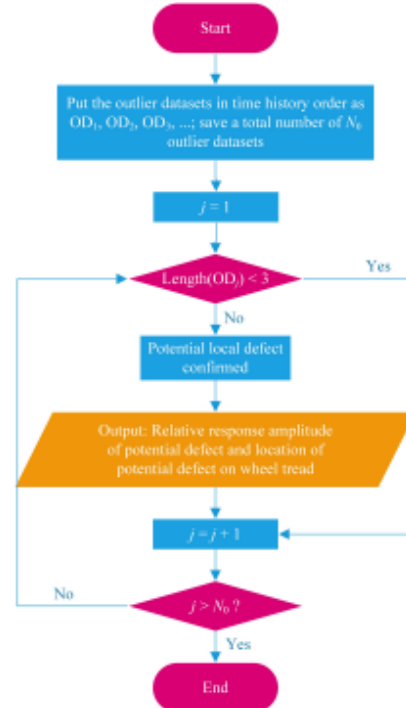
As shown in Fig. 5(a), the output strain data contain the major trend that reflects the variation of strain at rail base during the wheel passage, as well as disturbance caused by both wheel tread roughness and signal noise. By eliminating the major trend of raw data, the roughness of wheel tread can be better assessed. We apply the Savitzky-Golay (S-G) filter to smooth the strain data. By introducing 5-point quadratic polynomial to smooth the raw data for  $m$  times, the trend term of the strain data can be obtained. For a strain time series  $S_{(0)}$  ( $S_{(0)} = \{\varepsilon_1(0), \varepsilon_2(0), \dots, \varepsilon_n(0)\}$ ), the normalized

strain data  $S^*$  can be expressed as

$$S^* = S_{(0)} - S_{(m)} \tag{2}$$



(a) Main procedure



(b) Sub-process: confirmation of potential defect

Fig. 3 Procedure for wheel defect detection using online monitoring data of rail response

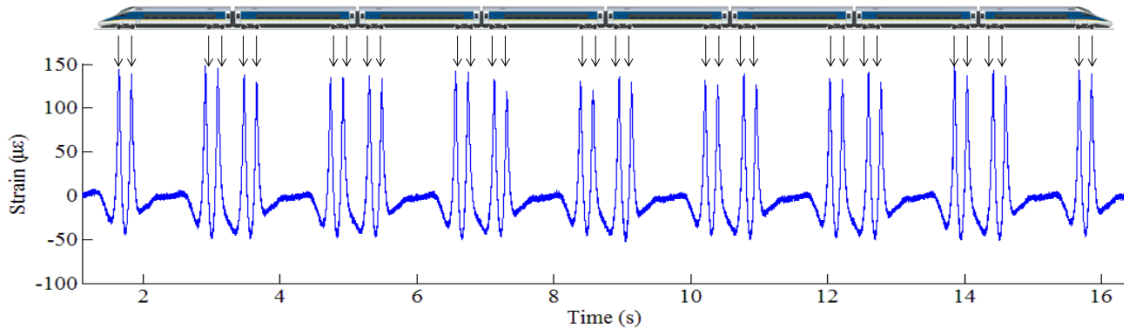
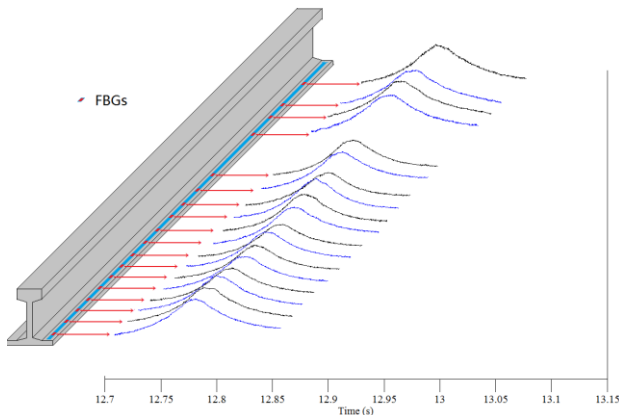


Fig. 4 Measured strain response by one FBG versus time

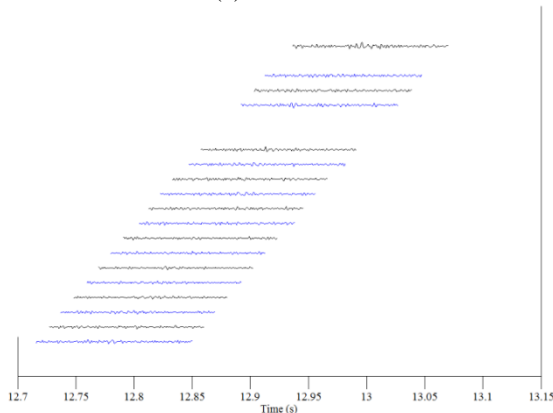
where  $S_{(m)}$  is the result after  $m$  times smoothing ( $m = 1, 2, \dots$ ) and it can be obtained as

$$S_{(m)} = AS_{(m-1)} = A^m S_{(0)} \quad (3)$$

where  $A$  is the matrix of coefficients specified by 5-point quadratic polynomial, as given by Savitzky and Golay (1964). Using the data smoothing technique, the relative measured strain response of the rail is obtained as shown in Fig. 5(b).



(a) Raw data



(b) Normalized data

Fig. 5 Strain responses from all FBGs excited by one wheel

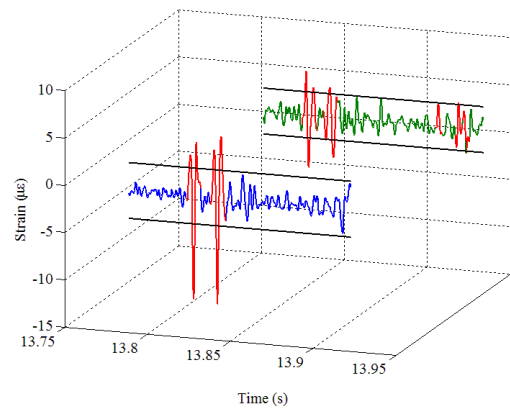
### 3.3 Localized response identification

It is seen that the normalized data are approximately normally distributed. If a Gaussian probability density function (PDF) is assigned to the data, the PDF parameters  $\mu$  and  $\sigma$  can then be obtained and updated by the growth of monitoring data collected by each FBG. Considering that the wheel defects rarely occur, the Chauvenet's criterion is a suitable outlier analysis approach in this situation. For given  $\mu$  and  $\sigma$ , a threshold for judging outliers from the normalized data can be set. The upper and lower limits of the probability band given by the Chauvenet's criterion are expressed in Eqs. (4) and (5), respectively.

$$x_u = F^{-1}(1 - 0.25/N | \mu, \sigma) \quad (4)$$

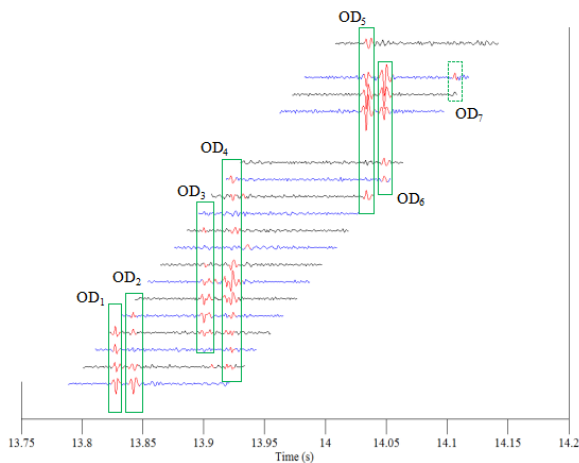
$$x_l = 2\mu - F^{-1}(1 - 0.25/N | \mu, \sigma) \quad (5)$$

where  $x_u$  and  $x_l$  are the upper and lower limits of the probability band,  $F^{-1}$  is the normal inverse function, and  $N$  is the sample size.



**Note:** Blue and green curves denote the normalized strain time history responses from two different FBGs; Black straight lines denote the upper and lower thresholds specified by the Chauvenet's criterion; Red curves denote the novel responses identified by outlier analysis.

Fig. 6 Outlier analysis of normalized strain data: an example of two strain response datasets



#### Outlier dataset information:

- OD<sub>1</sub>**: 4 novel responses, defect excitation time: 13.83s
- OD<sub>2</sub>**: 4 novel responses, defect excitation time: 13.84s
- OD<sub>3</sub>**: 6 novel responses, defect excitation time: 13.90s
- OD<sub>4</sub>**: 10 novel responses, defect excitation time: 13.92s
- OD<sub>5</sub>**: 5 novel responses, defect excitation time: 14.03s
- OD<sub>6</sub>**: 5 novel responses, defect excitation time: 14.05s
- OD<sub>7</sub>**: 1 novel response, defect excitation time: 14.12s

Fig. 7 Extraction of rail response monitoring data for wheel defect detection ( $N_0=7$ )

Given the lower and upper limits, outliers on the time history of the normalized strain data can be easily located and the novel responses that are likely excited by potential wheel defects can be drawn, as shown in Fig. 6. Note that here outliers are the data points beyond the lower or upper limits, and the outlier-centric strain responses are defined as novel responses.

#### 3.4 Detection of potential local defects

In Sub-section 3.3, the novel responses are obtained from outlier analysis. But whether the novel responses come from wheel defect still need further investigation because: 1) the monitoring data contain signal noise generated from the sensory system and other environmental interference, so some abnormal data may be falsely recognized as outliers; 2) the upper and lower thresholds given by outlier analysis is a screening mechanism rather than being used to identify wheel defect and the data points exceeding the thresholds are viewed as outliers instead of the sign of wheel defects. It is found in the previous studies that another necessary condition for the existence of wheel defect is that the novel responses from several strain gauges occur at the same time period. In view of this, we can scan the normalized strain data along the time history and generate several datasets, each of which corresponds to a point in time, called defect excitation time, and consists of all the novel responses. These outlier datasets are denoted as  $OD_j$  ( $j = 1, 2, \dots, N_0$ ) where  $N_0$  is the number of outlier datasets in the monitoring data of a specific wheel. If in an outlier dataset, there are no less than three novel responses, these novel responses can be regarded as being caused by a potential wheel defect.

Fig. 7 shows a typical set of monitoring data that are excited by a wheel with potential defect. 7 outlier datasets are observed in the normalized strain response data collected by an FBG array. Each of the outlier datasets  $OD_1, OD_2, OD_3, OD_4, OD_5$  and  $OD_6$  consists of no less than three novel responses and thus these novel responses can be viewed as being caused by potential defects. On the contrary,  $OD_7$  has only one novel response detected by the FBG, so it is screened out of defect detection.

## 4. In-situ verification

### 4.1 In-situ test

To verify the monitoring system and defect detection method, we chose an 8-car high-speed EMU (Fig. 8) as the test train. Some wheels with artificial local defects were installed on the EMU, but the defects were blind to us before the test. The train was instructed to run on the instrumented rail at five different speed levels: 10, 20, 30, 40 and 50 kph, respectively. At each speed level, the train ran four times. Thus we obtained 20 monitoring datasets for each wheel.

The detection method proposed in Section 3 is used to detect potential local defects from the monitoring data collected by the online WILD developed in Section 2. The wheel tread defect detection results will then be compared with the results of offline wheel inspection conducted later in the depot, as shown in Fig. 9. The analysis of detection results and validation of the wheel condition monitoring system including the defect detection method will be detailed in Sub-sections 4.2 and 4.3.

### 4.2 Wheel defect detection results

With the defect detection method developed in Section 3, the wheelsets with potential defects can be detected, as listed in Table 1. Both the left wheel and right wheel of wheelsets No. 1, 6, 24 and 27 are identified having potential defects, as indicated by most of the monitoring datasets. Besides, the left wheel of wheelset No. 23, the right wheel of wheelsets No. 7, 11, 13, 28 and 29 are detected as defective wheels but each of the wheels is detected by no more than three datasets (the total number of datasets is 20).



Fig. 8 An 8-car EMU running on instrumented rail



Fig. 9 Offline wheel tread inspection: left panel - radius deviation measurement; right panel - local defect detected

By comparing the online defect detection results with the offline radius deviation test results listed in right-hand columns of Table 1, it is found that the right wheels of wheelsets No. 1, 6, 24 and the left wheel of wheelset No. 27 are the wheels with local defects and they are all successfully detected in most of the tests, especially when the train ran at higher speed levels. Fig. 10 shows the defect detection results by the online monitoring and the radius deviation by offline inspection for the above four wheels, respectively. It can be seen that the defect detection results by the online monitoring system match well with the radius deviation measurement results for most of the local defects, in terms of both location and depth of the defect. Also, the defects whose depths are as low as 0.05~0.06 mm are identified from the detection results.

However, the wheels on the opposite side of the defective wheels which are identified by several online tests as “with defects”, are actually non-defective wheels, as indicated by the offline radius deviation inspection. This is because the defective wheel can affect the dynamic behavior of the whole wheelset including the wheel on the opposite side, which can then generate novel excitations on the rail; and the FBG array deployed on that rail can detect the novel responses caused by the defective wheel on the opposite side. This phenomenon has also been seen in the previous study (Barke and Chiu 2005) which revealed that the wheel on one side of the bogie as the impacting wheel and the wheel on the opposite side of the wheelset both experience rapidly fluctuating forces of smaller magnitude during the impact of a flat-defect wheel. Other potential defects found by online tests are all false alarms caused by unknown factors. Analysis of the detection error and detection accuracy will be given in Sub-section 4.3.

#### 4.3 Performance analysis in online detection

As the test train passed the instrumented rail section for 4 times at each running speed level, the number of defect detection tests is 256 under each train speed condition. Among the 256 samples, 16 are later proved to be “with defects” while 240 are “without defects”. It should be noted that among the 240 samples, 16 correspond to the wheels on the opposite side of defective wheels and the reason for a high opportunity of these wheels likely to be recognized as defective wheels has been explained in Sub-section 4.2.

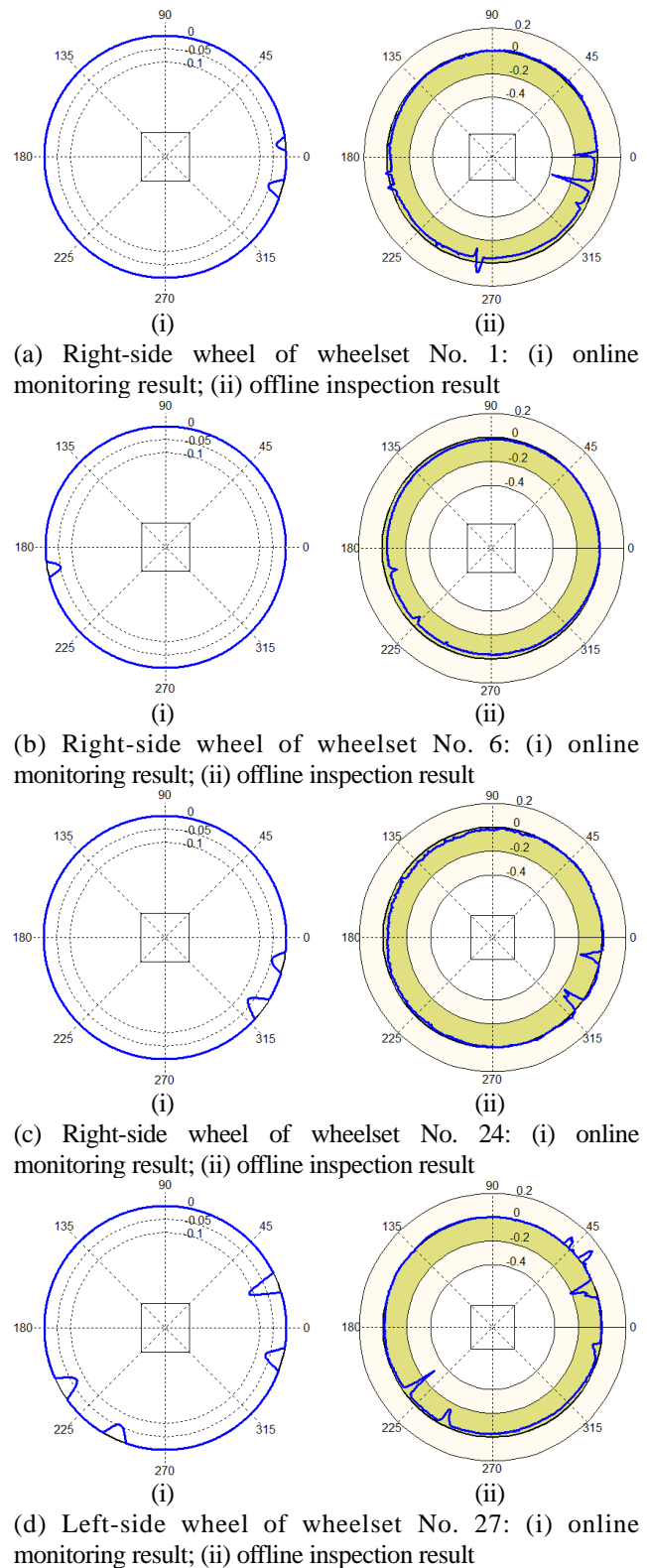


Fig. 10 Online wheel defect detection results verified by offline wheel radius deviation measurement

Table 1 Online defect detection results and offline inspection results for wheel tread

Wheelset No.	Side	Defect detection results (from online monitoring data)					Offline inspection results (from radius deviation test in depot)					
		Number of monitoring datasets from which defects are detected*					Number of defects	Depth of actual wheel tread defects (unit: mm)				
		10kph	20kph	30kph	40kph	50kph		Defect 1	Defect 2	Defect 3	Defect 4	
1	Left	0	0	2	2	1	0	(no defect)				
	Right	2	4	4	4	4	2	0.353	0.195	-	-	
6	Left	0	1	1	1	1	0	(no defect)				
	Right	0	2	4	4	4	2	0.062	0.056	-	-	
7	Right	0	1	0	0	0	0	(no defect)				
11	Right	0	1	0	0	1	0	(no defect)				
13	Right	0	0	0	0	1	0	(no defect)				
23	Left	0	0	1	2	0	0	(no defect)				
24	Left	0	0	0	0	2	0	(no defect)				
	Right	2	4	4	4	4	2	0.191	0.176	-	-	
27	Left	2	4	4	4	4	4	0.207	0.294	0.125	0.057	
	Right	0	2	4	4	4	0	(no defect)				
28	Right	0	0	1	0	0	0	(no defect)				
29	Right	0	0	0	0	1	0	(no defect)				

\* The total number of tests for each running speed level is 4

Table 2 Errors, error rates and accuracy of online wheel defect detection

		10 kph	20 kph	30 kph	40 kph	50 kph	Total
Error	False positive errors <sup>1</sup>	0	5	9	9	11	34
	False positive errors <sup>2</sup>	0	2	2	2	3	9
	False negative errors	10	2	0	0	0	12
Error rate	Type I error rate <sup>1</sup>	0%	2.1%	3.8%	3.8%	4.6%	2.8%
	Type I error rate <sup>2</sup>	0%	0.9%	0.9%	0.9%	1.3%	0.8%
	Type II error rate	62.5%	12.5%	0%	0%	0%	15%
Detection accuracy	Accuracy <sup>1</sup>	96.1%	97.3%	96.5%	96.5%	95.7%	96.4%
	Accuracy <sup>2</sup>	95.8%	98.3%	99.2%	99.2%	98.8%	98.3%

<sup>1</sup>: Including all 240 samples later proved "without defects";

<sup>2</sup>: Including 224 samples (the wheels on the opposite side of defective wheels are excluded from the 240 samples)

To analyze the detection accuracy of the proposed wheel load detector and defect detection method, we count all the false positive errors in the 1200 tests (240 for each running speed level), the false positive errors in 1120 tests (224 for each running speed level) where the samples from wheels on the opposite side of defective wheels have been excluded, and the false negative errors in 80 tests (16 for each running speed level), as shown in Table 2. The rates of type I and type II errors and the detection accuracy are also listed in the table. It is seen that as the train running speed increases, the type I error rate increases while the type II error decreases. The capacity of the detection method is highly related to the train running

speed when it is 30 kph or lower. But when the train speed is higher than 30 kph, all the defective wheels can be satisfactorily detected and only few false positives occur. It is hence concluded that the proposed wheel defect detection method has a high accuracy for wheel local defect detection when the train passes the instrumented rail section at running speeds of 30 - 50 kph.

## 5. Conclusions

This paper develops an FBG-based track-side wheel tread defect detection system and the corresponding data-based detection method for application to high-speed trains. As a track-side WILD, the proposed system is more suitable for large quantity of wheel inspections. By using fiber optic sensing technique, the system accounts for multiple FBG layouts and allows for remote monitoring. The data-based wheel defect detection method can automatically identify the rail responses in connection with the excitation generated by each wheel, normalize the collected data by a smoothing technique, detect the novel responses caused by potential defective wheels, and finally localize wheel defects. The effectiveness of the proposed system and detection method is verified by an in-situ test and the results indicate that the proposed detection method offers a high accuracy in wheel local defect detection when the train running speed is higher than 30 kph.

## Acknowledgments

The work described in this paper was supported by the funding from the Research Grants Council of the Hong Kong Special Administrative Region, China (Grant No. PolyU 152024/17E). The authors would also like to appreciate the funding support by the Ministry of Science and Technology of China and the Innovation and Technology Commission of Hong Kong SAR Government to the Hong Kong Branch of Chinese National Rail Transit Electrification and Automation Engineering Technology Research Center (Grants No. 2018YFE0190100 and K-BBY1).

## References

- Asplund, M., Famurewa, S. and Rantatalo, M. (2014), "Condition monitoring and e-maintenance solution of railway wheels", *J. Qual. Maint. Eng.*, **20**(3), 216-232.
- Baeza, L., Roda, A., Carballeira, J. and Giner, E. (2006), "Railway train-track dynamics for wheel flats with improved contact models", *Nonlinear Dynam.*, **45**(3-4), 385-397.
- Barke, D. and Chiu, W. K. (2005), "Structural health monitoring in the railway industry: a review", *Struct. Health Monit.*, **4**(1), 81-93.
- Bian, J., Gu, Y. and Murray, M. H. (2013), "A dynamic wheel-rail impact analysis of railway track under wheel flat by finite element analysis", *Vehicle. Syst. Dyn.*, **51**(6), 784-797.
- Ding, J., Lin, J., Wang, G. and Zhao, J. (2014), "Time-frequency analysis of wheel-rail shock in the presence of wheel flat", *J. Traffic Transp. Eng. (English Edition)*, **1**(6), 457-466.
- Ding, Y., An, Y. and Wang, C. (2016), "Field monitoring of the train-induced hanger vibration in a high-speed railway steel arch bridge", *Smart Struct. Syst.*, **17**(6), 1107-1127.
- Filigrano, M. L., Corredera, P., Rodríguez-Plaza, M., Andrés-Alguacil, A. and González-Herráez, M. (2013), "Wheel flat detection in high-speed railway systems using fiber Bragg gratings", *IEEE Sens. J.*, **13**(12), 4808-4816.
- Johansson, A. and Nielsen, J. C. (2003), "Out-of-round railway wheels—wheel-rail contact forces and track response derived from field tests and numerical simulations", *Proc. Instn. Mech. Engrs., Part F: Journal of Rail and Rapid Transit*, **217**(2), 135-146.
- Lagnebäck, R. (2007), "Evaluation of wayside condition monitoring technologies for condition-based maintenance of railway vehicles", Ph.D. Dissertation, Luleå Tekniska Universitet, Luleå.
- Milković, D., Simić, G., Jakovljević, Ž., Tanasković, J. and Lučanin, V. (2013), "Wayside system for wheel-rail contact forces measurements", *Measurement*, **46**(9), 3308-3318.
- Morys, B. (1999), "Enlargement of out-of-round wheel profiles on high speed trains", *J. Sound Vib.*, **227**(5), 965-978.
- Müller-BBM (2015), "Wheel roughness measuring device m|wheel", Müller-BBM Rail Technologies GmbH, München, Germany. Available at: <http://www.muellerbbm-rail.com/products/wheel-roughness-measuring-device/>
- Ni, Y.Q. (2015), "SHM-enriched high speed rail systems", *Proceedings of the 10th International Workshop on Structural Health Monitoring*, Stanford, California, USA.
- Ni, Y.Q., Ying, Z.G. and Liu, X.Z. (2017), "Online detection of wheel defect by extracting anomaly response features on rail: analytical modelling, monitoring system design, and in-situ verification", *Proceedings of the 14th International Conference on Railway Engineering*, Edinburgh, UK.
- Nielsen, J.C. and Oscarsson, J. (2004), "Simulation of dynamic train-track interaction with state-dependent track properties", *J. Sound Vib.*, **275**(3), 515-532.
- Petersson, M. (2000), "Noise-related roughness of railway wheel treads—full-scale testing of brake blocks", *Proc. Instn. Mech. Engrs., Part F: Journal of Rail and Rapid Transit*, **214**(2), 63-77.
- Pieringer, A., Kropp, W. and Nielsen, J. C. (2014), "The influence of contact modelling on simulated wheel/rail interaction due to wheel flats", *Wear*, **314**(1), 273-281.
- Savitzky, A. and Golay, M.J. (1964), "Smoothing and differentiation of data by simplified least squares procedures", *Anal. Chem.*, **36**(8), 1627-1639.
- Wei, C., Xin, Q., Chung, W.H., Liu, S.Y., Tam, H.Y. and Ho, S.L. (2012), "Real-time train wheel condition monitoring by fiber Bragg grating sensors", *Int. J. Distrib. Sens. N.*, **8**(1), 409048.
- Wei, X. and Chen, J. (2013), "Study on wheel-flat detection method based on vehicle system acceleration measurement", *Proceedings of the International Conference on Measurement, Information and Control (ICMIC)*, IEEE, Harbin, China.
- Wu, T.X. and Thompson, D.J. (2002), "A hybrid model for the noise generation due to railway wheel flats", *J. Sound Vib.*, **251**(1), 115-139.
- Yang, J. and Thompson, D. J. (2014), "Time-domain prediction of impact noise from wheel flats based on measured profiles", *J. Sound Vib.*, **333**(17), 3981-3995.
- Ye, X. W., Yi, T.H., Su, Y.H., Liu, T. and Chen, B. (2017), "Strain-based structural condition assessment of an instrumented arch bridge using FBG monitoring data", *Smart Struct. Syst.*, **20**(2), 139-150.
- Zhang, X., Liang, D., Zeng, J. and Lu, J. (2014), "SVR model reconstruction for the reliability of FBG sensor network based on the CFRP impact monitoring", *Smart Struct. Syst.*, **14**(2), 145-158.
- Zhao, X., Li, Z. and Liu, J. (2012), "Wheel-rail impact and the dynamic forces at discrete supports of rails in the presence of singular rail surface defects", *Proc. Instn. Mech. Engrs., Part F: Journal of Rail and Rapid Transit*, **226**(2), 124-139.